Controlling acoustic streaming in an ultrasonic heptagonal tweezers with application to cell manipulation

Controlling Acoustic Streaming in an Ultrasonic Heptagonal Tweezers with Application to Cell Manipulation

A.L. Bernassau, P. Glynne-Jones, F. Gesellchen, M. Riehle, M. Hill, D.R.S. Cumming

Abstract: Acoustic radiation force has been demonstrated as a method for manipulating micron-scale particles, but is frequently affected by unwanted streaming. In this paper the streaming in a multi-transducer quasi-standing wave acoustic particle manipulation device is assessed, and found to be dominated by a form of Eckart streaming. The experimentally observed streaming takes the form of two main vortices that have their highest velocity in the region where the standing wave is established. A finite element model is developed that agrees well with experimental results, and shows that the Reynolds stresses that give rise to the fluid motion are strongest in the high velocity region. A technical solution to reduce the streaming is explored that entails the introduction of a biocompatible agar gel layer at the bottom of the chamber so as to reduce the fluid depth and volume. By this means, we reduce the region of fluid that experiences the Reynolds stresses; the viscous drag per unit volume of fluid is also increased. Particle Image Velocimetry data is used to observe the streaming as a function of agar-modified cavity depth. It was found that, in an optimised structure, Eckart streaming could be reduced to negligible levels so that we could make a sonotweezers device with a large working area of up to 13 mm x 13 mm.

Keywords: Ultrasonic tweezers, Eckart streaming, Acoustic velocity, Particle trapping, Cell patterning, Manipulation.

I. INTRODUCTION

Techniques that allow the manipulation of cells and micro particles by non-invasive means are highly desirable so as to enable biological applications such as microarrays [1] and tissue engineering [2]. Non-invasive techniques exploiting the acoustic radiation forces have been demonstrated for trapping [3-10], separating [11-15] and rotating particles [16, 17]. In a standing wave field, the radiation force drives the particles into acoustic pressure nodes or/antinodes depending on their acoustic contrast factor [18]. However, other unwanted ultrasound-induced effects may disturb the distinct and precise manipulation or aggregation of suspended

particles. Acoustic streaming is one such phenomenon, characterised by time dependant flow patterns caused by the absorption of acoustic energy at both the boundaries of the device and in the bulk of the fluid. Three types of acoustic streaming [19-21] can affect the particle handling: Rayleigh streaming [22], Schlichting streaming, and Eckart streaming [23]. Rayleigh streaming creates vortices on the scale of $\lambda/4$ [24], moving the particles away from the pressure nodes and therefore influencing particle trapping [25]. Schlichting streaming can occur together with Rayleigh streaming, and forms a vortex with a thickness comparable to the viscous penetration depth at the boundary of the device. In contrast to Schlichting and Rayleigh streaming, which are driven by absorption in the viscous boundary layer, Eckart streaming is caused by the absorption of the acoustic energy in the bulk of the fluid [26]. It has been shown that Eckart streaming can be minimised by reducing the size of the resonator or by designing a resonator containing acoustically transparent foils [7, 25].

Acoustic streaming in a microsystem is often viewed as a negative side-effect that needs to be minimised. For example, for cell patterning and engineering, acoustic streaming will affect the positioning of the cells, possibly preventing the cells from adhering to the surface upon which they are growing. In our work [27-30], standing waves were created by interference of two propagating waves. Substantial disturbance of particle manipulation within the acoustic nodes was observed. The particles were constrained to nodal lines, but were driven along those lines by apparent streaming. Under these conditions, it was difficult to pattern particles in a reliable manner.

In this paper, we show that Eckart streaming is the mechanism causing the disturbance and that it is highly dependent on the height of the liquid contained in the cavity. The streaming can be greatly diminished if the depth of the liquid in the cavity is reduced. We present a quantitative study of the Eckart streaming that occurs in a heptagonal particle-manipulating device, also known as a "sonotweezer", and examine the case when two transducers are excited simultaneously. In order to precisely characterize the particles' behaviour we performed computer image analysis using particle image velocimetry (PIV) of the particle movement as a function of time. We have developed a finite element model of the Eckart streaming and have used it to confirm that this is the mechanism for the generation of streaming in the device, and to identify the regions where the driving force is strongest. It is found that the acoustic streaming is dependent on the depth of the sonotweezer cavity, and this phenomenon has been studied in detail by adding an agar layer at the bottom of the heptagonal cavity to vary the liquid depth without modifying the acoustic field. Agar has acoustic properties similar to water and does not change the acoustic wave interference patterns [31]. In this manner, the amount of liquid inside the cavity of the device was modified without disturbing the acoustic properties of the device. Agar was also found to be a highly

convenient filling material as it can be easily added and removed. In the newly configurable device that we present here, we are able to almost completely eliminate the effect of streaming so as to we create a large working area for a range of physical and biological experiments.

II. EXPERIMENTAL METHOD

The sonotweezers were made by bonding 5 x 5 x 0.5 mm NCE51 Noliac Ceramic lead zirconate titanate (PZT) (*E.P. Electronic Components Limited, UK*) plates to a flexible printed circuit board (10 x 72 mm; *Flexible dynamics Ltd, UK*) and folding it into a heptagon (Fig. 1) that was stabilised by top and bottom plates with a milled heptagonal slot. Acoustic synchronisation between channels was achieved using an arbitrary waveform generator providing four output channels (*TGA12104, Aim and Thurlby Thandar Instruments, UK*) allowing independent control of the amplitude, phase and frequency. The signals from the waveform generators were amplified by the low output impedance, high-speed, BUF634T buffer (*Texas Instruments, USA*).

The characterisation and the influence of the excited transducers has been investigated and discussed elsewhere [27]. It was found that when two transducers were excited particles were trapped along lines perpendicular to the bisecting vector of the normal to the planes of the transducers (Fig. 2). The combination where the activated transducers were adjacent to each other was shown to be less effective in trapping than the combination where at least one inactive transducer separates the active transducers. Adjustment of the relative phase difference between the active transducers allowed controlled movement of the position lines of particles in the direction of the bisecting vector.

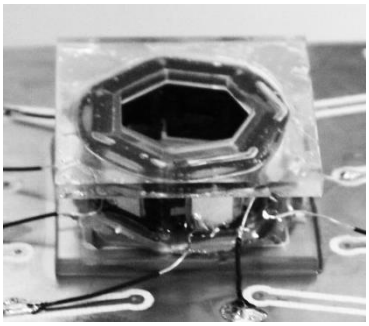

Fig. 1. Device shaped into a heptagon and bonded to a PCB to ease the connection of each channel (cell size ~ 2 cm).

In this paper two transducers (1-3) as shown in Fig. 2 were activated. The activation of the two transducers results in a field that has an array of linear traps in the centre of the cavity. The field pattern shown in Fig. 2 was obtained using a simulation based on 2D lines of point sources that sum up to form plane waves according to Huygen's principle [27].

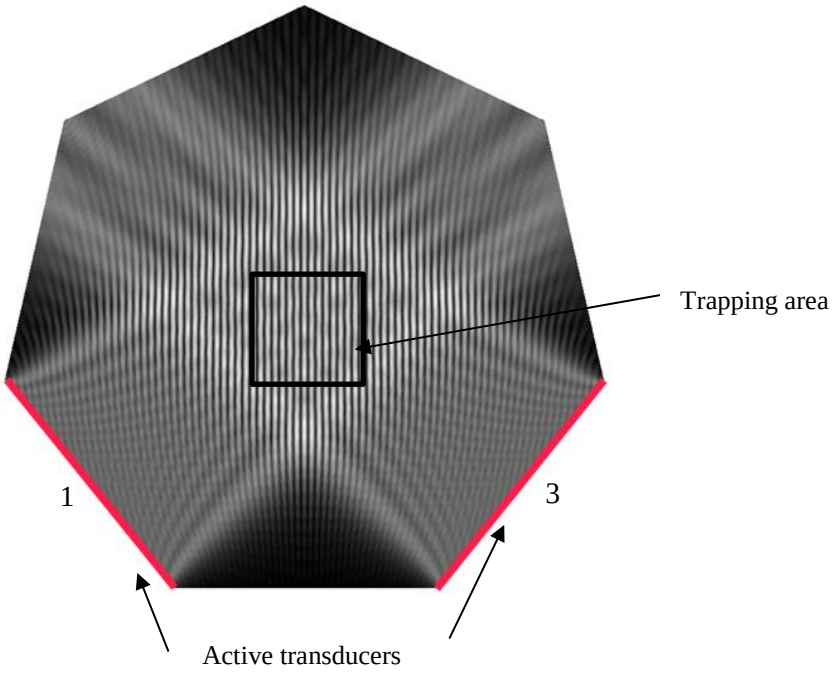

Fig. 2. Modelling results showing the quasi-standing waves formed in the centre of the heptagonal cavity when two transducers are excited simultaneously. The energy maxima are white, and the energy minima are black.

Fig. 3 shows 10 µm diameter polystyrene particles (*Polysciences Europe, Germany*) trapped at the nodes of the acoustic field in the centre of the cavity when two transducers, as shown in Fig. 2, are excited with continuous sine waves at an amplitude of 8 V_{pp} and a frequency of 4.00 MHz. For this data the device had no agar in place, and as discussed, streaming along the lines of particles was observed.

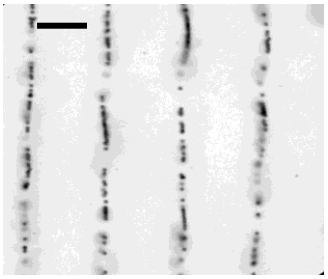

Fig. 3. Micrograph of the trapping area at the centre of the cavity showing trapping pattern when the transducers (1-3) were active. Scale bar = 200 µm.

III. FINITE ELEMENT MODELLING

A. Radiation Force

The Huygen's principle based method used to obtain Fig. 2 is not capable of modelling the streaming effect. In order to simulate streaming we require a detailed finite-element model for the acoustic fields. In order to develop such a model we must adequately describe the acoustic properties of the aqueous media.

When a particle is in an acoustic standing wave, the non-linear phenomenon of acoustic radiation causes a time-averaged force to act upon it, forcing the particle to either trap at the pressure node or antinode, depending on its acoustic contrast factor. The primary radiation force acting on a particle in an acoustic standing wave field was determined by King [32] and more generally by Gorkov [33], Eq. 1 [34]:

$$F(\boldsymbol{r}) = \nabla V\left(\frac{3\left(\rho_p - \rho_f\right)}{\left(2\rho_p + \rho_f\right)}E_{kin}\left(\boldsymbol{r}\right) - \left(1 - \frac{\beta_p}{\beta_f}\right)E_{pot}\left(\boldsymbol{r}\right)\right) \qquad \text{Eq. 1}$$

where V is the volume of a sphere located at position $\boldsymbol{r}$ within an acoustic field, characterized by its time averaged kinetic and potential energy densities (E_{kin} and E_{pot} respectively). The energy density terms are weighted by functions of the compressibilities (β_p and β_f) and densities (ρ_p and ρ_f) of the particle and the surrounding fluid respectively.

The primary force is strongly dependant on the particle size and frequency, thus as the particle diameter or frequency increase, the acoustic force increases rapidly. Most commonly found solid particles and cell types will be forced to the pressure nodes by the primary acoustic force, whereas, due to their low density and compressibility, lipid particles are moved towards a pressure antinode [35, 36].

When multiple particles are trapped in a standing wave, they not only experience the primary acoustic force, but also forces that are due to the scattered waves from the other particles. These inter-particle forces [37] are called secondary acoustic radiation forces. The secondary acoustic forces between two particles, Eq. 2, can be expressed in a simplified form [38]:

$$F_s(x) = 4\pi a^6\left[\frac{(\rho_c - \rho_w)^2(3\cos^2\theta - 1)}{6\rho_w d^4}v^2(x) - \frac{\omega^2\rho_w(\beta_c - \beta_w)^2}{9d^2}p^2(x)\right] \qquad \text{Eq. 2}$$

where a is the radius of the particle, d the distance between the particles and θ is the angle between the centre line of the particles and the direction of the propagation of the incident acoustic wave. The first term of Eq. 2 depends on the velocity amplitude of the particles, $v(x)$. The second term depends on the acoustic pressure

amplitude *p(x).* The secondary forces are usually weak and only active when the distance between particles is very small, such as in aggregation and sedimentation [39].

When an acoustic wave is present, acoustic streaming will also be occur, which will induce a Stokes drag force. The Stokes drag force can be expressed:

$$F_{drag} = -6\pi\mu a v \qquad \text{Eq. 3}$$

where a is the radius of the particle, μ the shear viscosity coefficient of the medium, and v the particle speed.

B. Acoustic Streaming

Acoustic streaming has been introduced by Lighthill [26] and based on early Nyborg and Westervelt's [40, 41] work. Eckart streaming can be express in terms of Reynolds stress, using an averaging operation over the Navier-Stokes equation to account for turbulent fluctuation in fluid momentum. Lighthill's equation (4) expresses this Reynolds stress, F_j, in terms of the j^{th} acoustic intensity component, I_j, an acoustic absorption coefficient, β, and the speed of sound, c:

$$F_j = \frac{\beta I_j}{c} \qquad \text{Eq. 4}$$

Möller *et al.* [42] used the gradient of a function of the velocity field to find F_j. This required sufficient mesh density was to resolve the variation of the Reynolds stress over the period of the standing wave, and sufficient numerical accuracy to allow cancellation of the periodic components of the Reynolds stress. In contrast, the approach used in this work, by using the intensity formulation, tolerates a lower mesh density since the average Reynolds stress does not vary over the spatial period of a wavelength. By so doing we are able to reduce numerical complexity need to model a device with a size that is many wavelengths across.

A 2-dimensional finite element model was developed using COMSOL software. The simulation has two steps: initially, a linear acoustic step calculates the first order acoustic wave field within the manipulation device; then, a Navier-Stokes, creeping flow, step models the induced motion of the fluid, using the results from the first step to calculate the acoustic intensity field, and hence the Reynolds driving force. In the first step, the walls of the chamber are modelled as radiation boundary conditions to mimic the energy lost into the structure. While in practice a certain amount of reflection is expected, experiments show that this effect is small compared to the radiation forces generated from wave travelling directly from the transducer. The model exploits the symmetry of the problem, allowing only half the physical domain to be modelled. An incident pressure field was added to the boundary where the transducers were present to represent the excitation. Fig. 2 shows the amplitude of the

modelled acoustic pressure field. Given the low velocities found in the experiments, it is sufficient to model the fluid in the creeping-flow regime. The effect of fluidic drag from the bottom surface of the chamber was modelled by adding a drag term to the Reynolds stress body force that corresponded to the fluidic resistance of an open channel. Fig. 4(a) shows the directions of the Reynolds stresses predicted by eq. 4, and Fig. 4(b) the resulting fluid motion. As can be clearly seen, both the interference pattern and streaming motion is modelled.

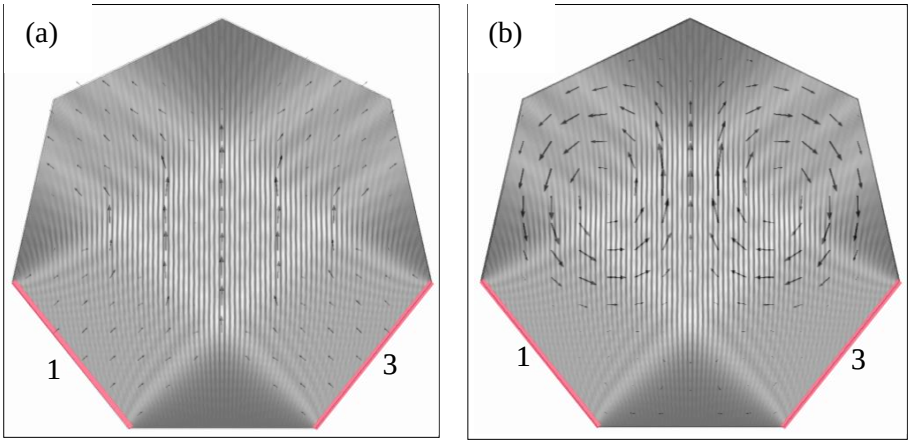

Fig. 4. (a) Modelled Reynolds stresses generated by the standing wave field and (b) the resulting streaming pattern. Both with arbitrary scale.

IV. RESULTS AND DISCUSSION

In the original, all liquid filled device, substantial particle movement was observed when the acoustic field was activated, and this was ascribed to streaming effects. It was found that the vortices that were created interfered significantly with the patterning of cells in the device. Under the influence of the streaming, the particles were driven along the lines of pressure nodes in which they were trapped (see Fig 4.). No transverse movement was observed across the lines. Because of the streaming it was difficult to form stationary patterns of particles using the original, unmodified, sonotweezers device.

Although we highlight applications for our device for cell manipulation, the experiments in this paper demonstrate manipulation with polystyrene micro-particles which have a more uniform size distribution. Our experience shows that 10 μm diameter polystyrene particles are a reasonable surrogate for many mammalian cells. This is supported by Augustsson *et al* [43] who present data for the acoustic contrast factor of a mesencephalic cell line finding contrast factors in the range 0.03 to 0.11 compared to the acoustic contrast factor for polystyrene micro-particles of 0.17 [44]. Since the acoustic force is proportional to the particle volume the smaller polystyrene particles are thus likely to experience forces of the same order of magnitude as the cells. At higher intensities ultrasound can create physiological effects, however several studies have investigated viability

and gene expression at intensities sufficient for manipulation in the MHz regime and found no observable changes even over extend periods of culture [45-48].

PIV experiments, described below, were used to produce Fig. 5 that shows that the circulation observed agrees qualitatively with the two counter-rotating streaming patterns predicted by the modelling (Fig. 4(b)). It is interesting to note that the majority of the Reynolds stresses are developed in the region where the plane-waves from the two transducers interfere. From the model we predicted that reducing chamber height would have the dual effect of reducing the amount of liquid experiencing the Reynolds stresses, and also increase the amount of viscous drag per unit volume of fluid that results from the boundary layer above the base of the device. We therefore conclude that an experimental implementation of the structure will lead to improved device performance.

Fig. 5. Particle Velocity Imaging of the fluid when transducers 1-3 are excited simultaneously.

In order to reduce the effective liquid depth, hence device volume, the cavity was partially filled. It was found that agar, having acoustic properties similar to those of water [31], is a good material for this function as it does not disturb the acoustic patterning capability of the device. Agar is also biocompatible, allowing cells or other biological material to be manipulated without harm, in the cavity.

Fig. 6 shows the behaviour and pattern of polystyrene particles (left) and Madin Darby Canine Kidney (MDCK) cells (right) with different heights of the agar layer deposited at the bottom of the device, allowing reduction of the cavity size and thus the "free" liquid quantity. Fig. 6 shows: (a) no agar layer or 1 cm height of liquid, (b) ¼ of the cavity filled with agar or 0.75 cm height of liquid, (c) ½ of the cavity filled with agar or 0.5 cm of liquid

and (d) ¾ of the cavity filled with agar or 0.25 cm of liquid. The corresponding volumes of DI water in each case were 2.0, 1.7, 1.0 and 0.6 mL respectively.

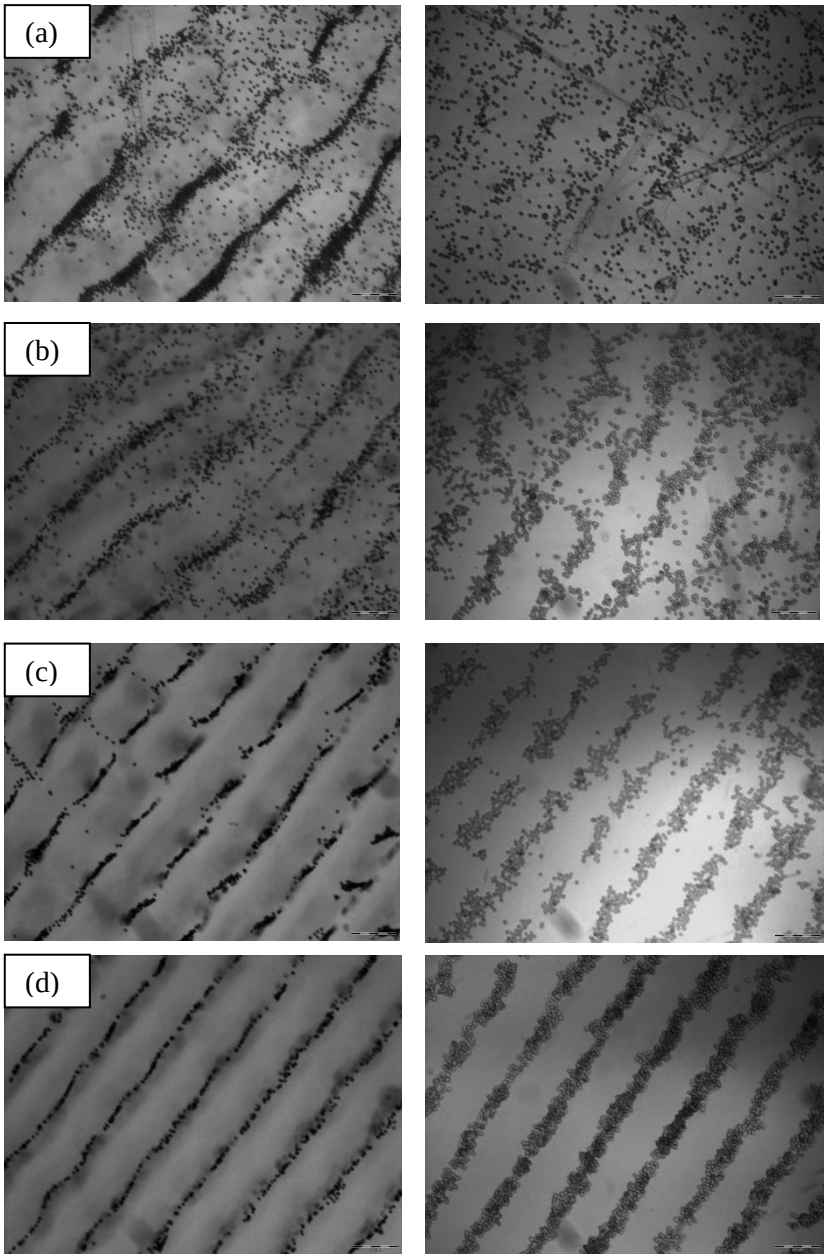

Fig. 6. Micrographs of the pattern of the particles(left) and cells (right) as a function of the height of the agar layer filling the cavity (a) 1 cm (b) 0.75 cm, (c) 0.5cm and (d) 0.25 cm.

The performance of the devices was studied in detail using PIV. All the PIV experiments were performed using 10, 6 and 1 μm diameter polystyrene particles (*Polysciences Europe, Germany*). The transducers were excited with 8 V_{pp} at a frequency at 4 MHz, as before. The 10 and 6 μm particles are susceptible to both the trapping and the bulk acoustic (streaming) forces. However, the 1 μm particles are too small to trap and therefore only

respond to the bulk acoustic forces. In this manner, we are able to use the behaviour of the differently sized particles to observe the effect of changing the cavity liquid depth on streaming. Exactly as for the experiment with results shown in Fig. 6, four depths of liquid were examined for their effect on Eckart streaming.

The concentration of particles in the DI water was the same for all the experiments and was approximately 4.5 x 10^6 particles/mL. Only one particle size was introduced to the device at any time. The concentration of particles into the DI water was selected to allow the trapping of a small number of particles, and to avoid the formation of large aggregates that are seen at higher concentrations. The sonotweezers device was placed on to a microscope stage under a 5x magnification objective lens (BX51, *Olympus UK Ltd, UK*). High resolution movies were acquired using a CMOS camera (*ORCA-flash 2.8, Hamamatsu, UK*). The movies were acquired in grey scale, at a rate of 45 frames/ s for 5s. Two movies, imaging two different areas of the trapping zone, were captured to ensure the reproducibility of the measurement process. The data is summarised in Table I and Fig. 8.

TABLE I. Velocity of particles vs. liquid heights

Liquid height in the cavity (cm)	Volume of DI water-particles in the cavity (mL)	Average Velocity (µm/s) 10 µm particles	Average Velocity (µm/s) 6 µm particles	Average Velocity (µm/s) 1 µm particles
1	2	150 ± 5.51	240 ± 5.95	300 ± 5.84
0.75	1.7	110 ± 4.25	200 ± 3.86	260 ± 3.73
0.5	1	65 ± 6.82	129 ± 5.85	190 ± 6.51
0.25	0.6	8 ± 0.33	17 ± 0.22	30 ± 0.29

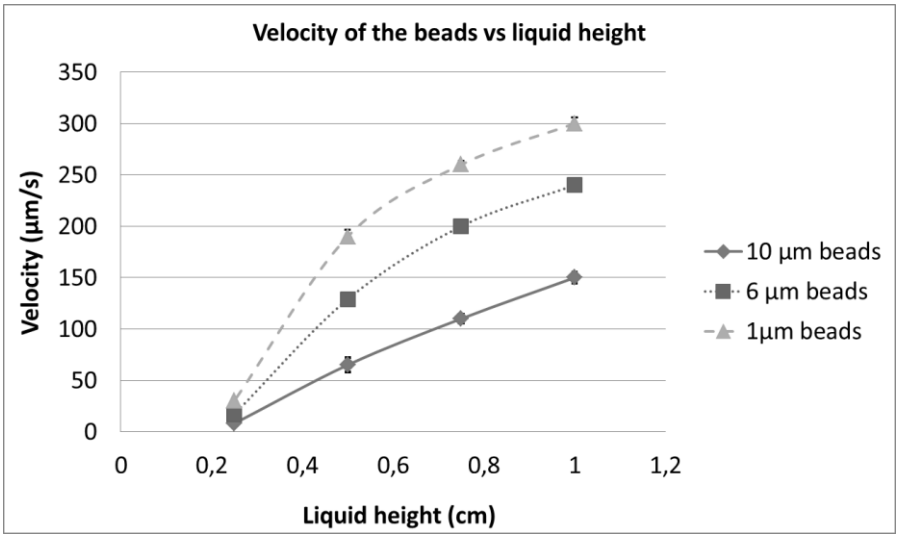

Fig. 8. Velocity of the particles vs the liquid heights in the heptagonal cavity.

The velocity measurements for 10, 6 and 1 µm showing the maximum velocity of the constrained particles in the trapping region (Fig. 3). The 10 and 6 µm particles are constrained and move along the nodal lines, and their movement is determined by contributions from both radiation forces and streaming drag forces. However, due to their small size the motion of 1 µm particles is predominantly determined by the acoustic streaming field, with little contribution from the radiation forces. It can be seen that with smaller volumes of liquid, the average of velocity of the particles decreases dramatically.

It can be seen that the average particle speed due to streaming is highly dependent on liquid height, with a very sharp reduction at the smallest depth. In going from no agar to 0.6 ml of liquid, the particle streaming is reduced by more than a hundred fold. Agar can be used as a possible solution to reduce the amount of liquid involve in the ultrasonic tweezers when the cavity cannot be physically reduced. It allows diminution of the acoustic bulk waves and thus allows excellent patterning of the cells.

Furthermore, measuring the acoustic field directly is difficult in this device since inserting a hydrophone will significantly distort the field. While numerical models give good predictions of field shapes, they are of limited value in predicting magnitudes since the amount of damping and absorption of energy that is transmitted into the device structure is very hard to predict or measure. In order to estimate the order of magnitude of the acoustic pressure, we examined the movement of 10 µm beads at 5 locations within the device using microscopy. The pair of transducers was excited at a frequency of 4 MHz and 8 Vpp. Beads velocities were in the range of 28 µm/s. The Stokes drag force, given by the Eq. 3 gives the acoustic radiation force required to produce the motion, we deduce that the acoustic pressure amplitude was approximately 71 kPa.

V. CONCLUSION

We have presented a method for reducing the amount of streaming in a counter-propagating wave type acoustic manipulation device whilst preserving the strength of the desired acoustic pattern. Finite element modelling has been shown effective in recreating the mechanism that leads to strong Eckart streaming in the region where the counter-propagating waves meet. The requirement in this type of device for transducers to be much larger than the required fluid volume (in order to avoid edge effects, and flexural modes) makes it hard to reduce the fluid volume of the cavity. However, the method we have devised overcomes this by the use of an agar gel deposited in the chamber. This method allows for the large manipulation area required in our application where cover slips are introduced into the tweezers. The agar has acoustic properties that are very similar to those of water, thus reduces the active region without disturbing the required acoustic resonance. This has been shown to reduce the unwanted streaming effects by two orders of magnitude to the point where they are negligible, enabling considerably improved cell patterning over a range of many wavelengths.

REFERENCES

[1] Flaim Christopher J, Chien Shu, and N. B. Sangeeta, "An extracellular matrix microarray for probing cellular differentiation," *Nat. Methods*, vol. 2, pp. 119-125, 2005.

[2] M. M. Stevens, M. Mayer, D. G. Anderson, D. B. Weibel, G. M. Whitesides, and R. Langer, "Direct patterning of mammalian cells onto porous tissue engineering substrates using agarose stamps," *Biomaterials*, vol. 26, pp. 7636-7641, 2005.

[3] W. T. Coakley, D. W. Bardsley, M. A. Grundy, F. Zamani, and D. J. Clarke, "Cell manipulation in ultrasonic standing wave fields," *Journal of Chemical Technology & Biotechnology*, vol. 44, pp. 43-62, 1989.

[4] J. Wu, "Acoustical tweezers," *The Journal of the Acoustical Society of America*, vol. 89, pp. 2140-2143, 1991.

[5] Y. Yamakoshi and Y. Noguchi, "Micro particle trapping by opposite phases ultrasonic travelling waves," *Ultrasonics*, vol. 36, pp. 873-878, 1998.

[6] J. J. Hawkes, D. Barrow, and W. T. Coakley, "Microparticle manipulation in millimetre scale ultrasonic standing wave chambers," *Ultrasonics*, vol. 36, pp. 925-931, 1998.

[7] H. M. Hertz, "Standing- wave acoustic trap for nonintrusive positioning of microparticles " *Journal of Applied Physics*, vol. 78, pp. 4845-4849, Oct 1995.

[8] P. Glynne-Jones, C. E. M. Demore, Y. Congwei, Q. Yongqiang, S. Cochran, and M. Hill, "Array-controlled ultrasonic manipulation of particles in planar acoustic resonator," *Ultrasonics, Ferroelectrics and Frequency Control, IEEE Transactions on*, vol. 59, pp. 1258-1266, 2012.

[9] J. Shi, D. Ahmed, X. Mao, S.-C. S. Lin, A. Lawit, and T. J. Huang, "Acoustic tweezers: patterning cells and microparticles using standing surface acoustic waves (SSAW)," *Lab on a Chip*, vol. 9, pp. 2890-2895, 2009.

[10] C. R. P. Courtney, C. K. Ong, B. W. Drinkwater, A. L. Bernassau, P. D. Wilcox, and D. R. S. Cumming, "Manipulation of particles in two dimensions using phase controllable ultrasonic standing waves," *Proceedings of the Royal Society A: Mathematical, Physical and Engineering Science*, vol. 468, pp. 337-360, 2012.

[11] O. Doblhoff-Dier, T. Gaida, H. Katinger, W. Burger, M. Groschl, and E. Benes, "A Novel Ultrasonic Resonance Field Device for the Retention of Animal Cells," *Biotechnology Progress*, vol. 10, pp. 428-432, 1994.

[12] E. Benes, M. Groschl, H. Nowotny, F. Trampler, T. Keijzer, H. Bohm, S. Radel, L. Gherardini, J. J. Hawkes, R. Konig, and C. Delouvroy, "Ultrasonic separation of suspended particles," *IEEE Ultrasonics Symposium*, vol. 1, pp. 649-659, 2001.

[13] H. Bohm, L. G. Briarty, K. C. Lowe, J. B. Power, E. Benes, and M. R. Davey, "Quantification of a novel h-shaped ultrasonic resonator for separation of biomaterials under terrestrial gravity and microgravity conditions," *Biotechnol Bioeng*, vol. 82, pp. 74-85, Apr 5 2003.

[14] J. Hu, J. Yang, J. Xu, and J. Du, "Extraction of biologic particles by pumping effect in a Ї€-shaped ultrasonic actuator," *Ultrasonics*, vol. 45, pp. 15-21, 2006.

[15] J. Shi, H. Huang, Z. Stratton, Y. Huang, and T. J. Huang, "Continuous particle separation in a microfluidic channel via standing surface acoustic waves (SSAW)," *Lab on a Chip*, vol. 9, pp. 3354-3359, 2009.

[16] J. Hu, C. Tay, Y. Cai, and J. Du, "Controlled rotation of sound-trapped small particles by an acoustic needle," *Applied Physics Letters*, vol. 87, 2005.

[17] X. Zhang, Y. Zheng, and J. Hu, "Sound controlled rotation of a cluster of small particles on an ultrasonically vibrating metal strip," *Applied Physics Letters*, vol. 92, 2008.
[18] T. Laurell, F. Petersson, and A. Nilsson, "Chip integrated strategies for acoustic separation and manipulation of cells and particles," *Chemical Society Reviews*, vol. 36, pp. 492-506, 2007.
[19] L. K. Zarembo, "Acoustic radiation pressure," in *High-intensity ultrasonic fields*, L. D. Rozenberg, Ed., 1971, p. 171.
[20] M. Wiklund, R. Green, and M. Ohlin, "Acoustofluidics 14: Applications of acoustic streaming in microfluidic devices," *Lab Chip*, vol. 12, pp. 2438-51, Jul 21 2012.
[21] M. Hill and N. R. Harris, "Chap. 9: Ultrasonic Particle Manipulation," in *Microfluidic Technologies for miniaturized Analysis Systems*, S. Hardt and F. Schonfeld, Eds.: Springer, 2007.
[22] L. Rayleigh, "On the Circulation of Air Observed in Kundt's Tubes, and on Some Allied Acoustical Problems," *Philosophical Transactions of the Royal Society of London* pp. 1-21, 1883.
[23] C. Eckart, "Vortices and Streams Caused by Sound Waves," *Physical Review*, vol. 73, pp. 68-76, 1948.
[24] N. Riley, "Acoustic Streaming," *Theoretical and Computational Fluid Dynamics*, vol. 10, pp. 349-356, 1998.
[25] J. Spengler and M. Jekel, "Ultrasound conditioning of suspensions - studies of streaming influence on particle aggregation on a lab- and pilot-plant scale," *Ultrasonics*, vol. 38, pp. 624-628, 2000.
[26] J. Lighthill, "Acoustic Streaming," *Journal of Sound and Vibration*, vol. 61, pp. 391-418, 1978.
[27] A. L. Bernassau, O. Chun-Kiat, M. Yong, P. G. A. Macpherson, C. R. P. Courtney, M. Riehle, B. W. Drinkwater, and D. R. S. Cumming, "Two-Dimensional Manipulation of Micro Particles by Acoustic Radiation Pressure in a Heptagon Cell," *Ultrasonics, Ferroelectrics and Frequency Control, IEEE Transactions on*, vol. 58, pp. 2132-2138, 2011.
[28] A. Bernassau, F. Gesellchen, P. MacPherson, M. Riehle, and D. Cumming, "Direct patterning of mammalian cells in an ultrasonic heptagon stencil," *Biomedical Microdevices*, vol. 14, pp. 559-564, 2012.
[29] F Gesellchen, AL Bernassau, DRS Cumming, and M. Riehle, "Cell manipulation using an acoustic tweezing device – Application in cell patterning and adhesion testing," in *European Cells and Materials*. vol. 23, 2012, p. 84.
[30] A. Bernassau, P. MacPherson, J. Beeley, B. W. Drinkwater, and D. Cumming, "Acoustic Patterning of Microspheres and Microbubbles in an Acoustic Tweezers," *Biomedical Microdevices*, vol. 15, pp. 289-297, 2013.
[31] K. Zell, J. I. Sperl, M. W. Vogel, R. Niessner, and C. Haisch, "Acoustical properties of selected tissue phantom materials for ultrasound imaging," *Physics in Medicine and Biology*, vol. 52, p. N475, 2007.
[32] L. V. King, "On the Acoustic Radiation Pressure on Spheres," *Proceedings of the Royal Society of London. Series A - Mathematical and Physical Sciences*, vol. 147, pp. 212-240, 1934.
[33] L. Gor'kov, "On the forces acting on a small particle in an acoustical field in an ideal fluid," *Soviet Physics-Doklady*, vol. 6, pp. 773-775, 1962.
[34] G. Whitworth and W. T. Coakley, "Particle column formation in a stationary ultrasonic field," *The Journal of the Acoustical Society of America*, vol. 91, pp. 79-85, 1992.
[35] A. L. Bernassau and D. R. S. Cumming, "Acoustic Tweezing in the Nodes or Antinodes of a Heptagonal Multi Piezoelectric Transducer Cell," *IEEE International Ultrasonics Symposium*, pp. 1537-1540, 2011.
[36] F. Petersson, A. Nilsson, C. Holm, H. Jonsson, and T. Laurell, "Separation of lipids from blood utilizing ultrasonic standing waves in microfluidic channels," *Analyst*, vol. 129, pp. 938-43, Oct 2004.
[37] V. F. K. Bjerknes, *Die Kraftfelder*: Braunschweig, 1909.
[38] M. A. H. Weiser, R. E. Apfel, and E. A. Neppiras, "Interparticle Forces on Red Cells in a Standing Wave Field," *Acta Acustica united with Acustica*, vol. 56, pp. 114-119, 1984.
[39] J. F. Spengler and W. T. Coakley, "Ultrasonic Trap To Monitor Morphology and Stability of Developing Microparticle Aggregates," *Langmuir*, vol. 19, pp. 3635-3642, 2012/07/18 2003.
[40] W. L. Nyborg, "Acoustic Streaming due to Attenuated Plane Waves," *Journal of the Acoustical Society of America*, vol. 25, p. 68, 1953.
[41] P. J. Westervelt, "The Theory of Steady Rotational Flow Generated by a Sound Field," *The Journal of the Acoustical Society of America*, vol. 25, pp. 60-67, 1953.
[42] D. Moller, T. Hilsdorf, J. Wang, and J. Dual, "Acoustic streaming used to move particles in a circular flow in a plastic chamber," *AIP Conference Proceedings*, vol. 1433, pp. 775-778, 2011.
[43] P. Augustsson, R. Barnkob, C. Grenvall, T. Deierborg, P. Brundin, H. Bruus, and T. Laurell, "Measuring the acoustophoretic contrast factor of living cells in microchannels," in *14. International Conference on Miniaturized Systems for Chemistry and Life Sciences* Groningen, The Netherlands, 2010, pp. 1337-1339.
[44] A. Lenshof, M. Evander, T. Laurell, and J. Nilsson, "Acoustofluidics 5: Building microfluidic acoustic resonators," *Lab on a Chip*, vol. 12, pp. 684-695, 2012.
[45] H. Bohm, P. Anthony, M. R. Davey, L. G. Briarty, J. B. Power, K. C. Lowe, E. Benes, and M. Groschl, "Viability of plant cell suspensions exposed to homogeneous ultrasonic fields of different energy density and wave type," *Ultrasonics*, vol. 38, pp. 629-632, 2000.
[46] D. Bazou, R. Kearney, F. Mansergh, C. Bourdon, J. Farrar, and M. Wride, "Gene Expression Analysis of Mouse Embryonic Stem Cells Following Levitation in an Ultrasound Standing Wave Trap," *Ultrasound in Medicine & Biology*, vol. 37, pp. 321-330, 2011.
[47] B. Vanherberghen, O. Manneberg, A. Christakou, T. Frisk, M. Ohlin, H. M. Hertz, B. Onfelt, and M. Wiklund, "Ultrasound-controlled cell aggregation in a multi-well chip," *Lab on a Chip*, vol. 10, pp. 2727-2732, 2010.
[48] J. Hultstrom, O. Manneberg, K. Dopf, H. M. Hertz, H. Brismar, and M. Wiklund, "Proliferation and viability of adherent cells manipulated by standing-wave ultrasound in a microfluidic chip," *Ultrasound Med Biol. 2007 Jan;33(1):145-51.*, vol. 33, pp. 175-181, 2006.